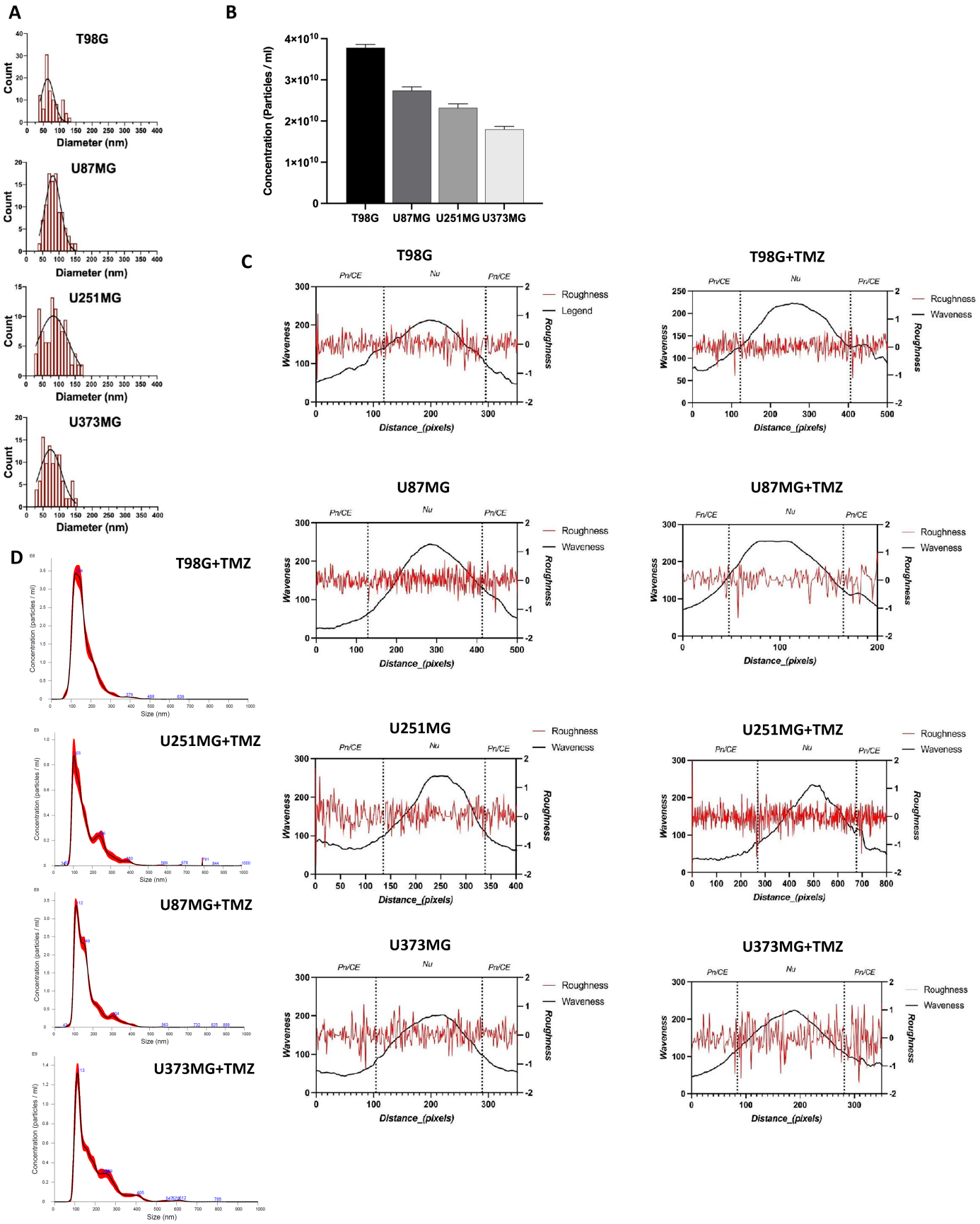
Supplementary Materials

Temozolomide reshapes concentration, morphology, proteome, and biological activity of glioblastoma-derived extracellular vesicles

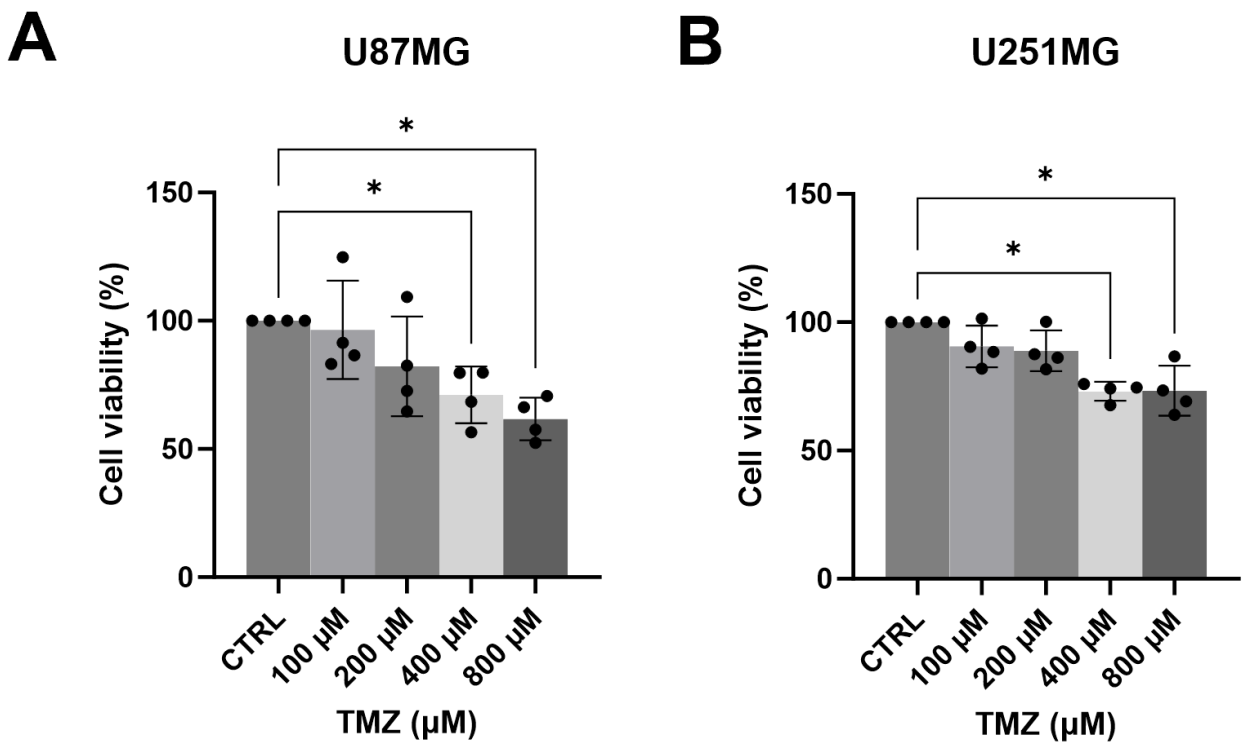
Diana Vardanyan[1,#], Mariana Karimova[2,#], Iulia Efimova[2,3], Federica Fratini[4], Simone Dinarelli[5], Maria Concetta Cufaro[6,7], Marcello Chieppa[8], Maurizio Zuccotti[9], Andrea Alfieri[10], Piero Del Boccio[7,11], Dmitri V. Krysko[2,3,†], Luciana Dini[1], Stefano Tacconi[1]

[1]Department of Biology and Biotechnologies "Charles Darwin", Sapienza University of Rome, Rome 00185, Italy.
[2]Cell Death Investigation and Therapy (CDIT) Laboratory, Anatomy and Embryology Unit, Department of Human Structure and Repair, Ghent University, Ghent 9000, Belgium.
[3]Cancer Research Institute Ghent, Ghent 9000, Belgium.
[4]Department of Neuroscience, Istituto Superiore di Sanità (ISS), Rome 00185, Italy.
[5]Institute for the Structure of Matter (ISM), National Research Council (CNR), Rome 00133, Italy.
[6]Department of Innovative Technologies in Medicine and Dentistry, G. d'Annunzio University of Chieti-Pescara, Chieti 66100, Italy.
[7]Center for Advanced Studies and Technology (CAST), Proteomics and Metabolomics Core Facility, G. d'Annunzio University of Chieti-Pescara, Chieti 66100, Italy.
[8]Department of Environmental and Biological Science and Technology, University of Salento, Lecce 73100, Italy.
[9]Department of Biology and Biotechnology "Lazzaro Spallanzani", University of Pavia, Pavia 27100, Italy.
[10]Centro Grandi Strumenti, University of Pavia, Pavia 27100, Italy.
[11]Department of Science, G. d'Annunzio University of Chieti-Pescara, Chieti 66100, Italy.
[#]These authors contributed equally to this work.
[†]In memoriam.

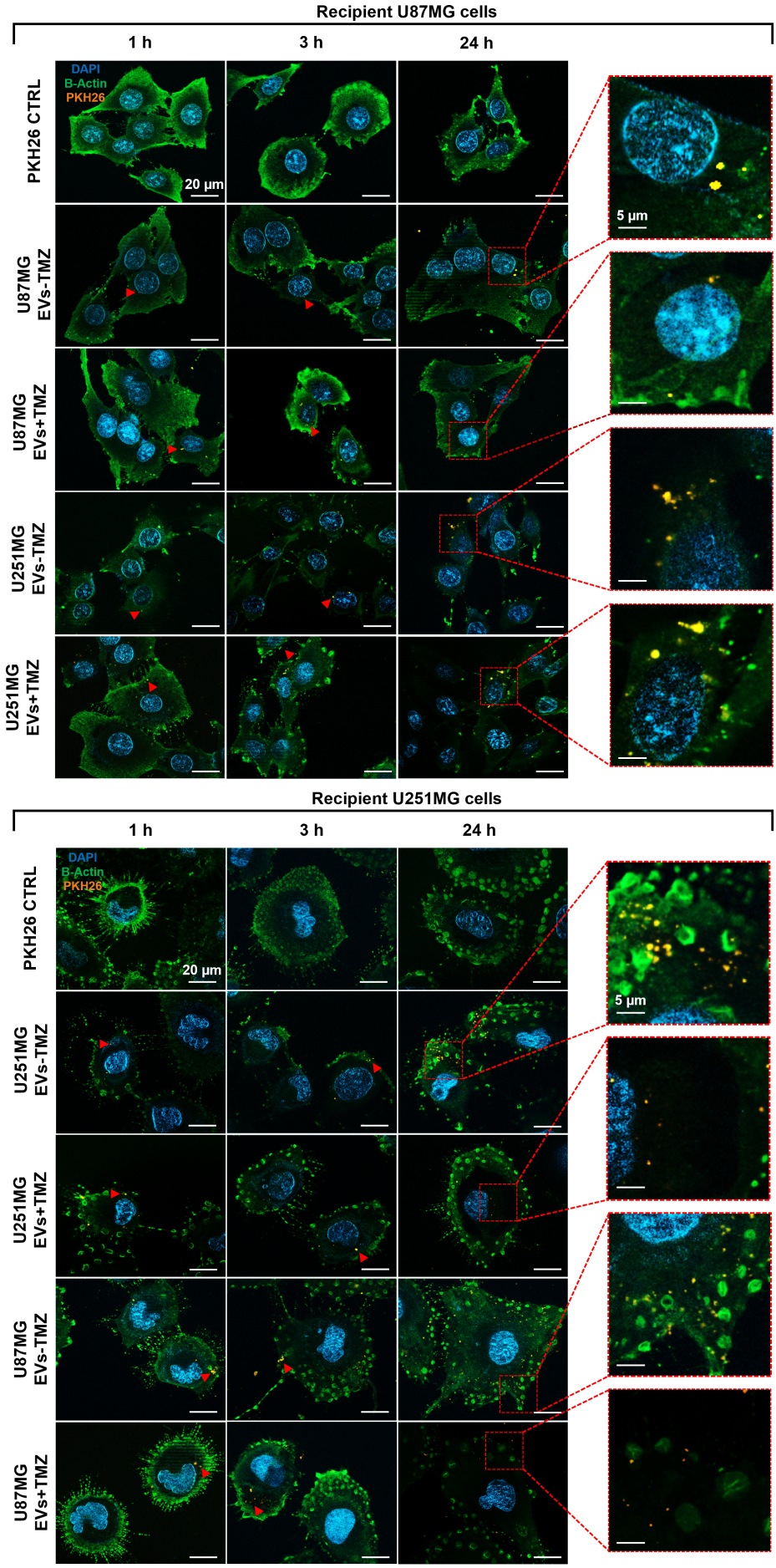
Correspondence to: Prof. Luciana Dini, Dr. Stefano Tacconi, Department of Biology and Biotechnologies "Charles Darwin", Sapienza University of Rome, Rome 00185, Italy. E-mail: luciana.dini@uniroma1.it; stefano.tacconi@uniroma1.it



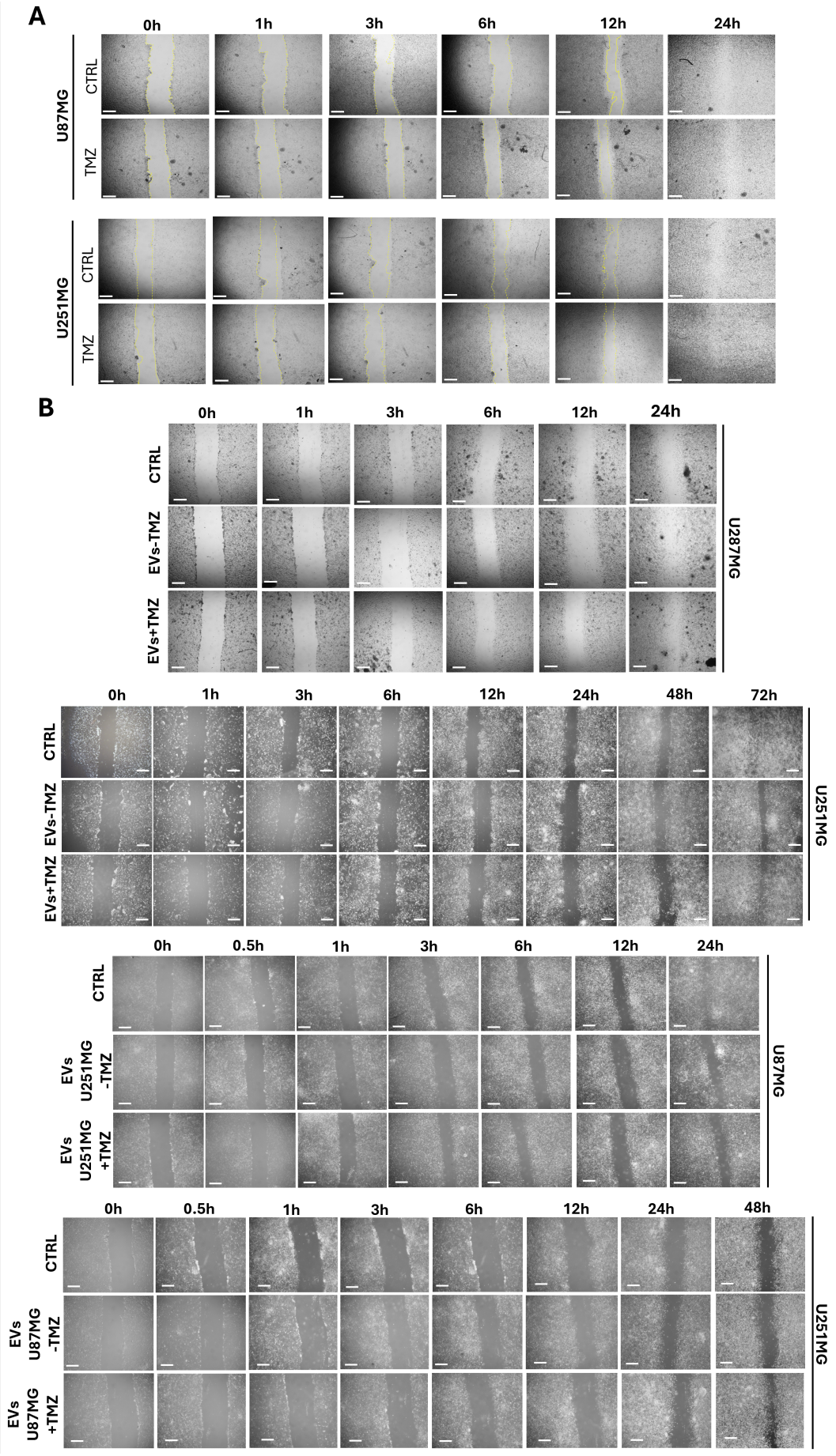
Supplementary Figure 1. Size distribution by TEM (A) and particle concentration by NTA (B) of EVs from T98G, U87MG, U251MG, and U373MG cells. (C) Representative profiles of roughness (red line) and waviness (black line) across untreated and TMZ-treated T98G, U87MG, U251MG, and U373MG cells. The black vertical dotted lines separate the nuclear (Nu) and perinuclear/cellular edge (PNu/CE) regions. (D) Size distribution of EVs isolated from TMZ-treated T98G, U251MG, U87MG, and U373MG cells measured by NTA.



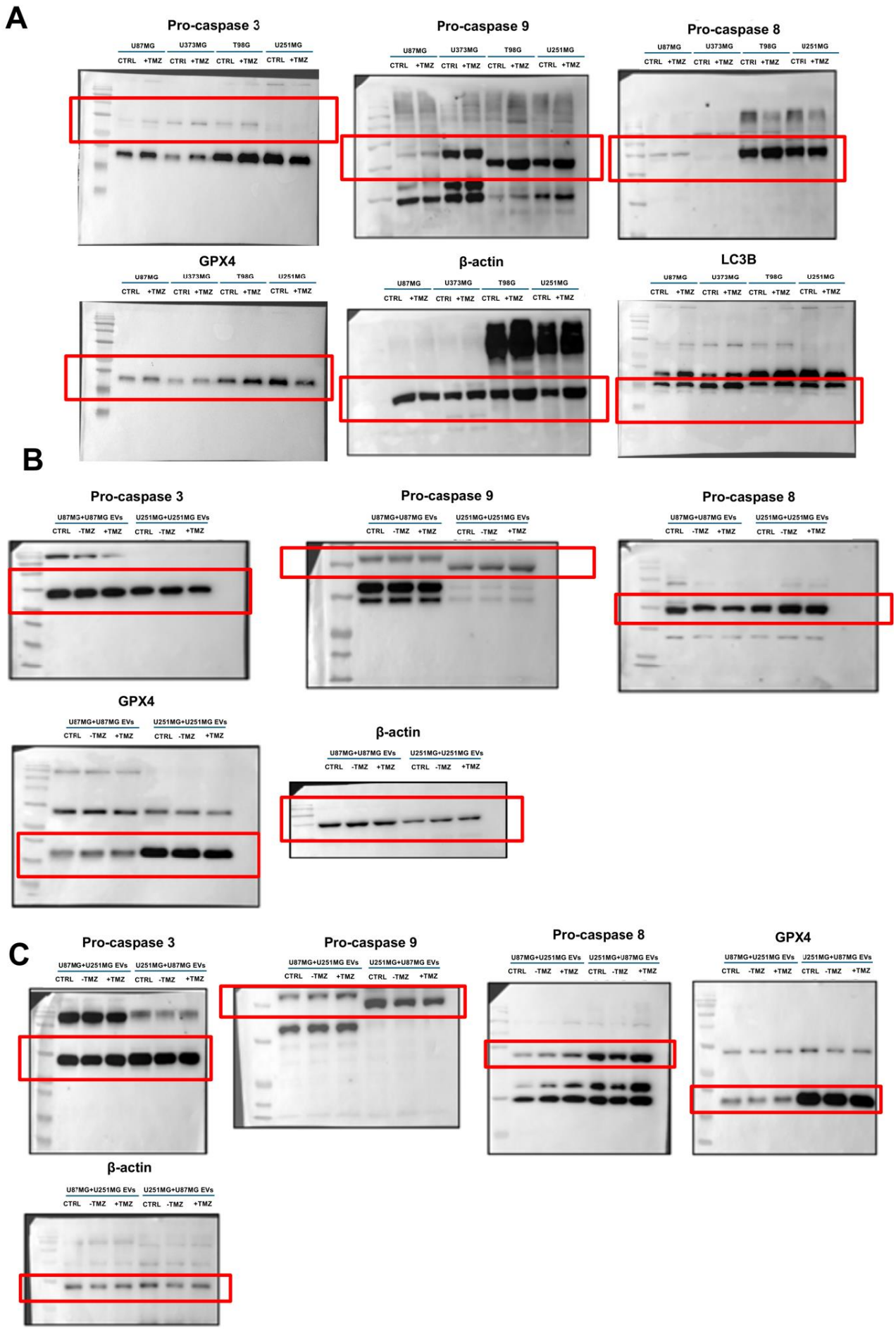
Supplementary Figure 2. Effect of TMZ on the viability of U87MG and U251MG cells assessed using a crystal violet assay. U87MG (A) and U251MG (B) cells were treated with 100, 200, 400, or 800 µM TMZ for 48 h. Data are reported as percentage compared to the control (untreated cells; CTRL) presented as mean ± SD of four individual biological replicates ($n = 4$). $^{*}P < 0.05$ *vs*. control (Student's *t*-test).



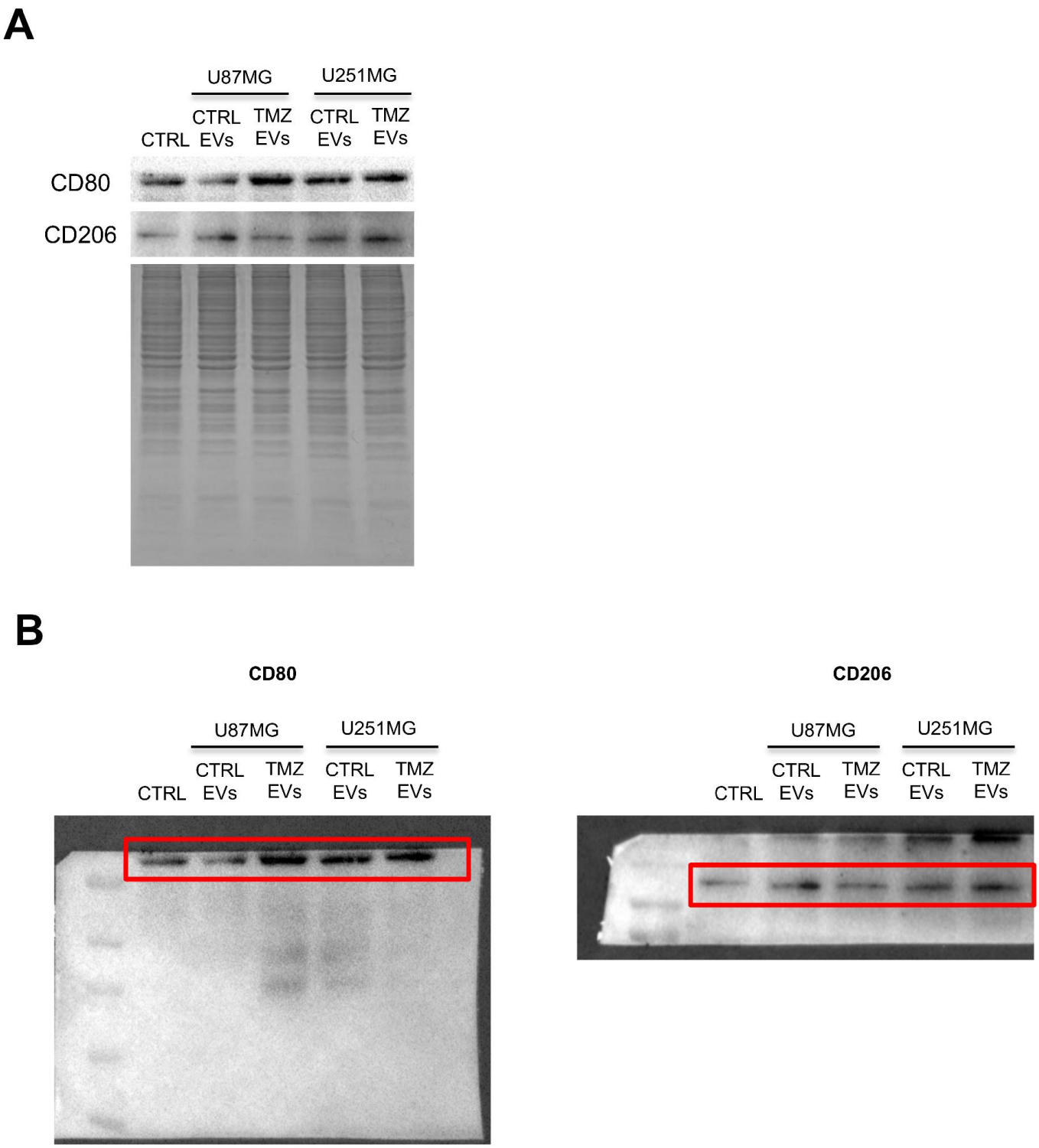
Supplementary Figure 3. Microscopy fluorescence images showing the uptake of PKH26-labelled EVs from untreated (EVs-TMZ) and TMZ-treated (EVs+TMZ) U87MG and U251MG cells in recipient GBM cells after 1, 3, and 24 h of incubation. PKH26-only controls (PKH26 CTRL) were included to confirm the absence of free dye.



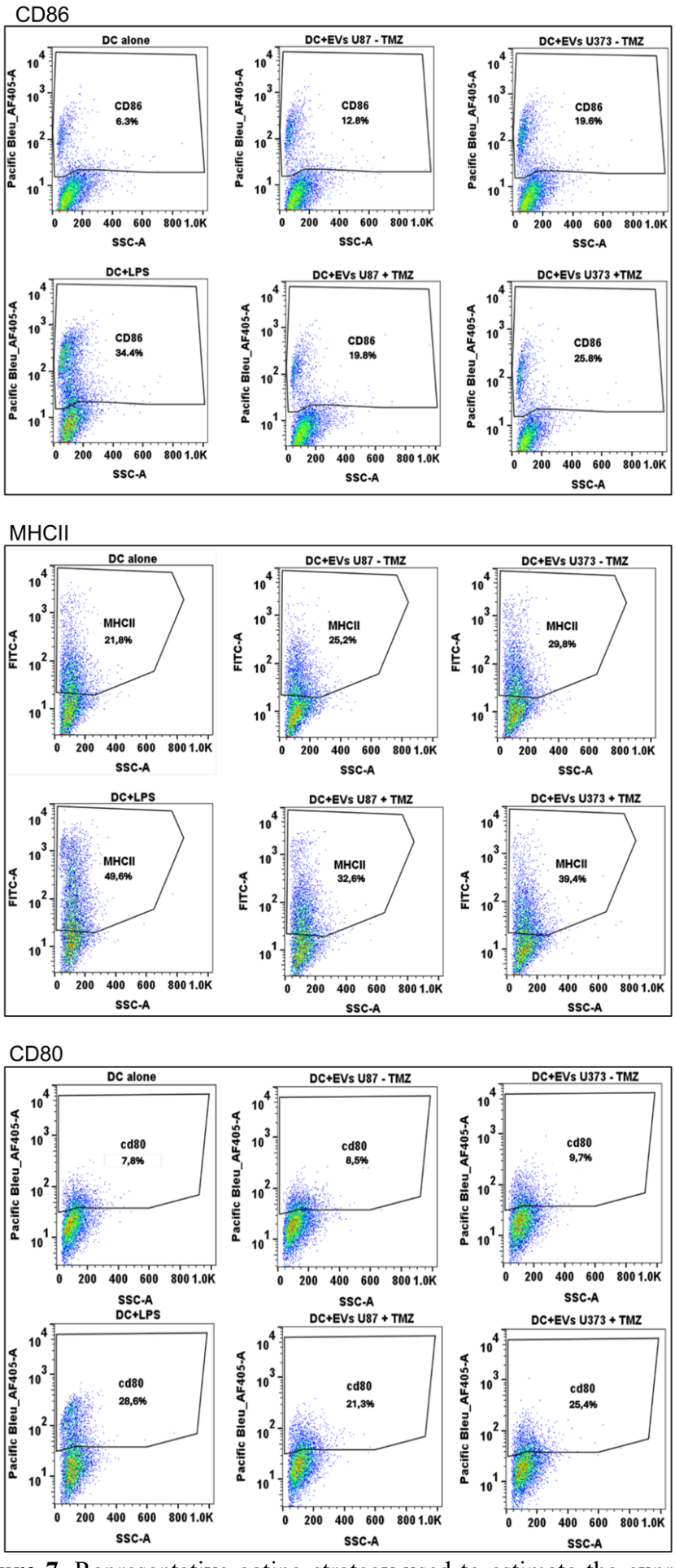
Supplementary Figure 4. (A) Representative bright field images of the wound healing assay performed on untreated (control, CTRL) and TMZ-treated U87MG and U251MG cells and reported in Figure 4B and C; (B) Representative bright field images of the wound healing assay performed on untreated and EV-treated U87MG and U251MG cells incubated with EVs derived from untreated and TMZ-treated U87MG and U251MG cells reported and in Figure 4D and E.



Supplementary Figure 5. Original uncropped Western blot images shown in Figure 5G (A) and 5K (B and C).



Supplementary Figure 6. (A) Representative Western blot images of CD80 and CD206 in BV-2 cells untreated (CTRL) and treated with EVs from untreated and TMZ-treated U87MG and U251MG cells. Ponceau red (bottom) was used as loading control. Original uncropped Western blot images are reported in (B).



Supplementary Figure 7. Representative gating strategy used to estimate the expression levels of CD86, MHCII, and CD80 by flow cytometry reported in Figure 6. First, cell debris was gated out, after which CD11c+ cells were selected. From CD11c+ population, CD86+, MHCII+ or CD80+ population was selected.

Supplementary Table 1. List of quantified and differential proteins.